INDIAN JOURNAL OF SCIENCE AND TECHNOLOGY

RESEARCH ARTICLE

OPEN ACCESS

Received: 29-06-2024

Accepted: 21-07-2024

Published: 06-08-2024

Citation: Mandal G, Bhattacharjee B (2024) RSM-CCD Modeling and Optimization for Adsorptive Removal of Rose Bengal Dye from Aqueous Medium using CeO_2 Nanoflowers. Indian Journal of Science and Technology 17(31): 3199-3209. https://doi.org/10.17485/IJST/v17i31.2122

* **Corresponding author**.

baib23@gmail.com

Funding: None

Competing Interests: None

Published By Indian Society for Education and Environment (iSee)

ISSN
Print: 0974-6846
Electronic: 0974-5645

RSM-CCD Modeling and Optimization for Adsorptive Removal of Rose Bengal Dye from Aqueous Medium using CeO_2 Nanoflowers

Goutam Mandal[1], Baibaswata Bhattacharjee[2]*

1 Department of Physics, Bankura Zilla Saradamani Mahila Mahavidyapith, Bankura, 722101, West Bengal, India
2 Department of Physics, Ramananda College, Bishnupur, 722122, West Bengal, India

Abstract

Objective: The focus of the study was to synthesize cerium oxide (CeO_2) nanoparticles (NPs) and use them as nano adsorbents to remove toxic Rose Bengal (RB) dye from wastewater. **Methods:** A simple chemical method was used to synthesize CeO_2 nanostructures. The nanostructures were characterized using XRD spectra, FESEM, and UV-Vis spectroscopy. The nanoparticles are used as nano adsorbents for wastewater treatment. Here, we utilized response surface methodology-central composite design (RSM-CCD) to optimize the batch adsorption studies rather than using the usual one-variable-at-a-time approach. The parameters for our investigations were the agitation period, CeO_2 NP dosage, solution pH, and initial RB dye concentration. **Findings:** The characterization study showed that nanoflowers of a mean particle size of 44 nm and band gap of 3.68 eV were formed. RSM-CCD methodology for optimization resulted in an agitation time of 29.36 min, an NP dose of 0.302 g/L, a solution pH of 6.96, and a starting dye concentration of 88.65 mg/L gives the highest adsorption of 88.46%. The kinetics data indicated a strong fit with the pseudo-second-order (PSO) equation, while the Freundlich isotherm model fitted the equilibrium data accurately, resulting in q_{max} =187 mg/g. The thermodynamic analysis suggested that adsorption was characterized by being endothermic, spontaneous, and physical. **Novelty:** The unique nanoflowers were employed and removal efficiency was predicted using a 2nd-order polynomial equation in Stat-Ease Design Expert Software ver.13. The model showed an excellent match with an adjusted R^2 value of 0.9736 and a projected R^2 value of 0.9256.

Keywords: Cerium oxide nanoparticles; Adsorption; Response surface methodology; Central composite design; Rose Bengal; Optimization

1 Introduction

The worldwide shortage of freshwater due to contamination of organic dyes threatens environmental conservation and human health. Wastewater from fabric, paper mills, and medicinal industries has residual dyes and other water pollutants [1].

Chemical waste from dye industries is a challenging problem due to its high chemical resistance and environmental stability. Waterborne infections and severe water pollution result from dye discharge [2]. Rose Bengal [$C_{20}H_4Cl_4I_4O_5$] is a xanthene dye used in the textile, dye, and photochemical industries. RB dyes exhibit great water solubility, leading to water pollution and significant toxicity to living organisms [3]. As a result, removing Rose Bengal (RB) from the effluent is essential before discharging it into the aquatic systems and protecting our environment and health [4]. Several physical, chemical, and biological approaches for organic dye elimination have been developed. However, every method is associated with restrictions, such as cost, complexity, and the effectiveness of the removal process. On the other, there is no doubt that adsorption is an easy, viable, efficient, and notable approach [5]. Researchers have attempted numerous adsorbents with various affinities to eliminate the dye and other contaminants from wastewater. Due to their unique features, nanoparticles have recently attracted substantial attention, and their application as adsorbents and photocatalysts has become a focus of extensive research [6].

Semiconductor metal oxide nanoparticles are often preferred over metal nanoparticles due to their easy fabrication, stable nature at high temperatures and a broad pH range, inexpensive costs, high porosity, and chemical and biological reactivity [7]. Among the others, cerium oxide nanoparticles have been the focus of many investigations conducted mainly because of their exceptional surface chemistry, prominent stability, and biocompatibility [8]. Nanoscale cerium oxide is a direct and wide band gap semiconductor [9]. Cerium is a rare earth element and the first metal in the lanthanide series of the periodic table. Cerium oxide nanoparticles containing 3+ and 4+ cerium on their surface have a wide range of industrial uses [10]. Although several studies have been conducted on CeO_2 NPs as photocatalysts, there is a lack of studies on their application as an adsorbent [11].

Considering all these, this study aims to synthesize CeO_2 NPs and consider their dye removal potential via the adsorption method. The microstructural properties of produced nanoparticles (NPs) were examined using an X-ray diffractometer, a FESEM, and a UV-Vis spectrophotometer. The study on adsorption examines the influences of various parameters, including dosage of adsorbent, agitation time, initial dye concentration, and solution pH. The optimization was done using the central composite design (CCD) and response surface methodology (RSM). In addition to this, adsorption kinetic, isotherm, and thermodynamics were also studied. Our findings indicated that the CeO_2 nanoflowers successfully removed RB dye through adsorption.

2 Methodology

2.1. Materials

All chemical reagents were of analytical grade and were utilized in their original form. Merck supplied cerium nitrate hexahydrate [$Ce(NO_3)_3.6H_2O$] and potassium carbonate [K_2CO_3]. The Rose Bengal dye was acquired from SRL, India. A stock solution of RB (1.0 g/L) was prepared, and subsequent dilutions were made using deionized water to reach the required final concentration.

2.2 Synthesis of the CeO_2 nano adsorbent

CeO_2 NPs were synthesized via the co-precipitation method at room temperature. A 0.05M, 100 mL cerium nitrate solution was ready by dissolving the stoichiometric amount of $Ce(NO_3)_3.6H_2O$ in deionized water. Similarly, 0.03M, 100 mL of potassium carbonate solution was prepared by dissolving K_2CO_3 in deionized water. At room temperature, aqueous potassium carbonate solution was added dropwise with cerium nitrate under stirring and continued overnight. A white precipitate of cerium carbonate was observed at the end. After filtering with filter paper, the precipitation obtained was cleaned with deionized water twice or thrice. Then, the final precipitation was dried in hot air at 60^0 C for about 3 h and calcined in a furnace at 600^0C for about 5 h. The final product was then dried for storage. Figure 1 depicts the synthesis process of the nano adsorbent.

2.3 Characterization techniques

We have recorded the X-ray diffraction (XRD) data in a Rigaku (Japan) made X-ray diffractometer (with Cu-Kα radiation and λ =1.54 Å) throughout an angular range of 20° to 80°. The absorption peak and band gap characteristics were studied using a UV-Vis spectrophotometer (Systronics AU 2703 double-beam) in the 200 to 800 nm wavelength range. A ZEISS-made FESEM was employed to analyze the surface morphology of the adsorbent at accelerating voltages of 5 kV.

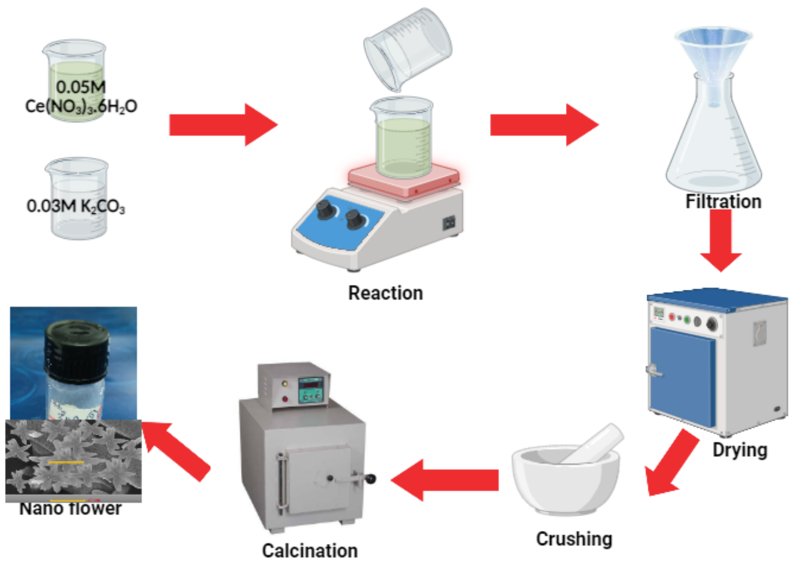

Fig 1. The process ofsynthesizing nano-adsorbent

2.4 Adsorption Study

The adsorption of RB dye onto CeO_2 was investigated in batch experiments. To attain the optimum conditions, the effect of the agitation period (10-60 min), adsorbent dosage (0.1-0.5 g/L), pH of the solution (5-9), and initial RB concentrations (30-150 mg/L) were assessed by RSM. The adsorption experiments were conducted in a 100 ml flask containing 50 ml of RB dye solution. The solutions were agitated in an orbital shaker before being separated by centrifugation for 15 min at 4000 rpm. The residual dye concentrations were determined using a UV-Vis spectrophotometer by studying the peak at 545 nm for RB dye. The pH of the solution was adjusted to be high or low with HCl or NaOH. The % removal of the RB dye was calculated using the following relation[12]:

Removal percentage

$$(\%) = \frac{C_i - C_e}{C_i} \times 100\% \tag{1}$$

The quantity of dye adsorbed (q_e), or adsorption capacity (mg/g) at equilibrium can be determined by the relation[13]:

$$q_e = \frac{C_i - C_e}{W} \tag{2}$$

Here, C_i: initial dye concentration, C_e: equilibrium dye concentration (mg/L), W: adsorbent's mass (g/L).

A calibration curve between concentration and amount of dye in mg/L was used to determine the amount of dye present in the solution.

2.5 Study of Adsorption Isotherm, Kinetic and Thermodynamics

Adsorption equilibrium experiments reveal the maximum amount of an adsorbate an adsorbent can take up. Langmuir and Freundlich isotherm models have been utilized in sorption isotherm studies of RB dye with CeO_2 NPs.

The isotherm model of Langmuir can be described as:

$$\frac{C_e}{q_e} = \frac{1}{q_{max K_L}} + \frac{C_e}{q_{max}} \tag{3}$$

Here, q_{max} : the maximum adsorption capacity (mg/g) and K_L: Langmuir constant (L/mg).

Freundlich adsorption model may be expressed in the linear form as:

$$logq_e = logK_F + \frac{1}{n} logC_e \tag{4}$$

Here, K_F: Freundlich constant $[(mg/g)(L/mg)^{1/n}]$and n: intensity parameter.

The process kinetics and adsorption rates are modeled using rate equations. The study of adsorption kinetics was done using the Lagergren pseudo-first-order (PFO) adsorption model and is represented in linear form as:

$$ln(q_t - q_e) = lnq_e - K_1 t \tag{5}$$

Where, K_1: PFO rate constant, and t : time of adsorption, q_t : amount of dye adsorbed at time t.

The pseudo-second-order (PSO) model can be written as:

$$\frac{t}{q_t} = \frac{t}{q_e} + \frac{1}{K_2 q_e^2} \tag{6}$$

Where, K_2: PSO rate constant, and t : time of adsorption.

The study of thermodynamic parameters, e.g., enthalpy (ΔH), entropy (ΔS), and standard free energy (ΔG), is vital to estimating the adsorption process's thermodynamic viability and spontaneous behavior. These are all obtained by applying the following equations:

$$\triangle G = \triangle H - T\triangle S \tag{7}$$

$$lnK_c = -\frac{\triangle H}{RT} + \frac{\triangle S}{R} \tag{8}$$

Where R: universal gas constant (8.314J/mol/K) and $K_c (= \frac{q_e}{C_e})$: adsorption equilibrium constant.

2.6 Experimental Design-Batch study and Statistical analysis (RSM)

The RSM combines statistical, experimental, and mathematical techniques for analyzing numerical data and their interaction in analytical studies. It can be used to design multivariate data, which leads to simultaneous equations and solves the same[14]. The central composite design (CCD) is a well-known RSM approach for design enhancement. The CCD estimates all linear, quadratic, and two-way interactions using a rotating lower dimensional design topology. A preliminary test was conducted to find the suitable ranges of independent process variables. Based on single factor experiments, a four variable CCD composed of agitation period (10-60 min), adsorbent dosage (0.1-0.5 g/L), pH of the solution (5-9), and initial RB concentrations (30-150 mg/L) was considered as the independent variable. In addition, the adsorption of RB dye was regarded as the response variable. The CCD was used to assess the level of the four independent parameters- agitation period (A), NP dose (B), solution pH (C), and RB initial concentration (D) (Table 1).

The RB removal (response) was predicted by Design-Expert software version 13 using a 2nd-order polynomial equation. The software did statistical analysis, which cut down on the number of tests that had to be done to find out how each measure controlled and interacted with the others. We compared the models to the experimental data using analysis of variance (ANOVA), and we used Fischer's F test to see if the interactions between the variables were statistically significant. The binary interactions were represented using three-dimensional surface graphs. The model employed optimization techniques to ascertain precise values for each independent variable and offer the most favorable adsorption conditions.

Table 1. Factors and their levels

Factors	Name	Units	Minimum	Maximum
A	Time	Min.	10.00	60.00
B	Dosage	g/L	0.1000	0.5000
C	pH		5.00	9.00
D	Concentration	mg/L	30	150

3 Results and Discussion

3.1.The characterization of the Adsorbent

A strong absorption peak of synthesized NPs was found at 362 nm at the UV -Vis spectra Figure 2**(A).** The Tauc plot (Figure 2(**B**)) calculated the direct excitonic band gap as 3.68eV. The FESEM characterized the surface morphology, and as shown in Figure 2**(C),** the image reveals that nanoflowers are formed. The powder XRD pattern of synthesized CeO_2 nanocrystal was mentioned in Figure 2 **(D)**. The peaks were observed at 2θ and (111), (200), (220), (311), (222), (400), (331), and (420) Miller planes, which can be indexed to the face centre cubic fluorite structure of nanoceria [15]. The nanocrystal depicted maximum peak intensity $2\theta = 28.761\ A^0$ of miller plane (111), which was utilized to calculate the crystallite size of 44.8 nm.

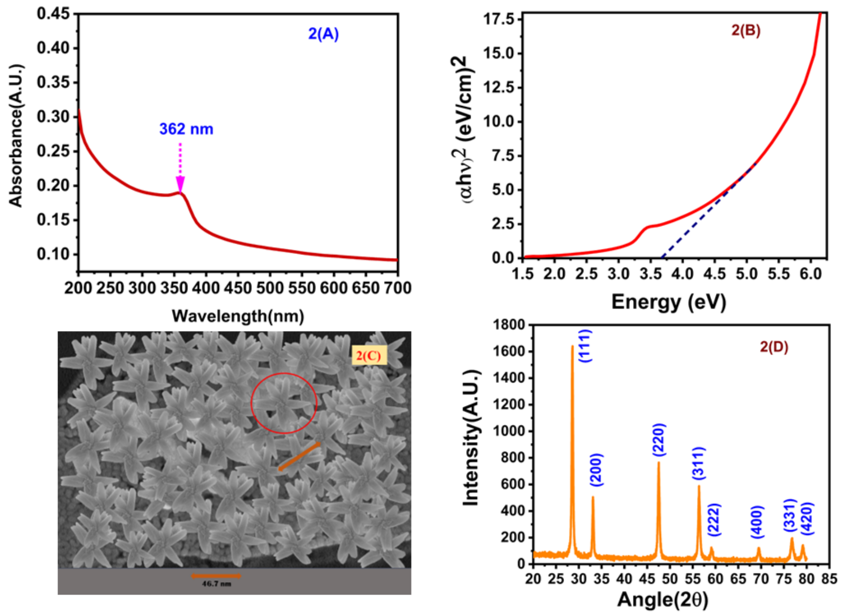

Fig 2. Characterization of the nano adsorbent- (A) The UV-Vis absorption spectra, (B) The Tauc plot to determine the band gap, (C) SEM images, and (D) XRD data plot

3.2 Adsorption Experiments

Optimization was performed using the one factor at a time (OFAT) experimental method. Adsorption of RB dye was investigated by varying the agitation times from 0 to 60 min in intervals of 5 min. The absorbent dosage was 0.3 g/L; the pH of the solution was 6, and the temperature was kept constant at 303 K. The adsorbent showed rapid initial adsorption, reaching saturation in about 35 min. The influence of adsorbent dosage on the dye removal efficiency of RB was investigated over a range from 0.1 to 0.6 g/L, while other conditions were kept constant. The highest rate of dye removal was 54.2%, which was obtained using an adsorbent dose of 0.3 g/L. The effect of pH on the adsorption of RB dye was investigated by altering the pH of the dye solution within the range of 4.0 to 9.0. The pH of 7.0 is optimal for the adsorption of RB by the adsorbent based on the measured pH circumstances. The effect of the initial dye concentration on the adsorption of RB dye on CeO_2 NPs was investigated across a range of 10-100 mg/L. The highest percentage of RB removal was 80.7% at 90 mg/L.

3.3 The Mathematical Modeling (RSM)

The impact of four independent factors on RB adsorption was investigated by employing a central composite design (CCD) to conduct 30 experimental runs: agitation duration (A), CeO_2 NP dose (B), solution pH (C), and RB dye initial concentration (D). The objective was to identify the principal interaction effects of these variables on the adsorption of RB dye. To reduce experimental errors, replicates were retained. The analysis of variance (ANOVA) was used to conduct a diagnostic test to determine the suitability of the suggested model, employing Fisher's F (lack of fit) test. The regression coefficient (R^2) quantifies the extent to which the model accounts for variance seen around the mean. The data from 30 CCD studies, including both coded and uncoded levels of independent components, are shown in Table 2. Using coded factors, the quadratic model may be represented as follows:

$$RB\ Removal = 88.45 - 0.6000A + 0.2000B + 0.0333C - 0.4333D + 2.4000AB + 19.1000AC + 7.4500AD - 5.1000BC - 3.7500BD - 2.0500CD - 17.7100A^2 - 21.7100B^2 - 13.6100C^2 - 14.4500D^2 \quad (9)$$

The coded factors equation can be employed to predict the reaction at different amounts of each factor. The coded equation helps determine the elements' relative impact by comparing their coefficients.

Table 2. Designed variables and the response

Run	Time (min)	Dosage (g/L)	pH	Initial concentration (mg/L)	Adsorptive (%)	Removal
1	10	0.3	7	90	72.3	
2	30	0.3	7	90	88.7	
3	20	0.2	6	60	76.4	
4	20	0.2	8	60	69.5	
5	20	0.4	8	120	61.8	
6	40	0.2	6	120	66.7	
7	30	0.3	9	90	74.5	
8	40	0.4	8	120	74.5	
9	20	0.2	6	120	75.6	
10	30	0.3	7	90	88.7	
11	30	0.3	7	90	88.7	
12	30	0.3	7	90	88.7	
13	30	0.3	7	30	74.5	
14	20	0.4	8	60	68.5	
15	20	0.4	6	60	80.2	
16	20	0.2	8	120	68	
17	40	0.2	8	60	75.6	
18	30	0.1	7	90	65.5	
19	40	0.4	8	60	75.8	
20	30	0.5	7	90	68.3	
21	20	0.4	6	120	72.6	
22	40	0.4	6	60	65.2	
23	30	0.3	7	90	88.7	
24	30	0.3	7	150	73.6	
25	50	0.3	7	90	69.5	
26	30	0.3	5	90	75.5	
27	30	0.3	7	90	87.2	
28	40	0.4	6	120	71.6	
29	40	0.2	6	60	62.3	
30	40	0.2	8	120	79.3	

3.3.1 Analysis of variance (ANOVA)

The ANOVA test showed that the model has a statistically significant F value of 77.48 (Table 3). The probability of such a high F value being due to noise is 0.01%. Model terms are considered statistically significant when the P-value is less than 0.0500. The critical model terms in this case are AC, AD, BC, BD, A^2, B^2, C, and D^2. Lack of fit is not statistically significant (F = 6.60) when compared to pure error. We aim for a minimal mismatch. The expected R^2 of 0.9256 and the adjusted R^2 of 0.9736 are close. Adeq Precision determines the signal-to-noise ratio. The signal-to-noise ratio is low, the design space is navigable, and the ratio is more than 4.

3.3.2 Response Surface Plots

Multiple 3D response graphs were exploited to collect data and to evaluate the importance of RB adsorption empirically. Factors include agitation time (A), CeO_2 NP dose (B), pH of the solution (C), and RB dye initial concentration (D). Figure 3**(A)** and **(B)** demonstrate that the adsorption of RB is enhanced by extending the contact duration. Initially, the adsorbent has many

Table 3. ANOVA table for quadratic model

Source	Sum of Squares	df	Mean Square	F-value	p-value	
Model	1924.32	14	137.45	77.48	< 0.0001	significant
A-Time	2.16	1	2.16	1.22	0.2872	
B-Dosage	0.2400	1	0.2400	0.1353	0.7181	
C-pH	0.0067	1	0.0067	0.0038	0.9519	
D-Initial concentration	1.13	1	1.13	0.6351	0.4379	
AB	5.76	1	5.76	3.25	0.0917	
AC	364.81	1	364.81	205.64	< 0.0001	
AD	55.50	1	55.50	31.29	< 0.0001	
BC	26.01	1	26.01	14.66	0.0016	
BD	14.06	1	14.06	7.93	0.0130	
CD	4.20	1	4.20	2.37	0.1446	
A^2	537.57	1	537.57	303.03	< 0.0001	
B^2	807.86	1	807.86	455.39	< 0.0001	
C^2	317.46	1	317.46	178.95	< 0.0001	
D^2	363.33	1	363.33	204.81	< 0.0001	
Residual	26.61	15	1.77			
Lack of Fit	24.73	10	2.47	6.60	0.0252	significant
Pure Error	1.87	5	0.3750			
Cor Total	1950.93	29				

active sites, but the dye molecules later take up these sites. The concentration of RB adsorption was constant when the contact duration was prolonged beyond 30 min, as seen in these figures. The adsorption of RB was considerably impacted by the solution pH Figure 3**(A)** and **(C)**. The initial dye concentration is also very important. A linear correlation exists between the initial RB concentration rise and the variance. As a result, the rise in initial RB concentration equals the rise in RB adsorption. Figure 3**(B)** and **(D)** show that increasing the initial RB concentration increases adsorption. The adsorption process is described in the Figure 3 **(E)**.

3.3.3 Optimization

The investigation focused on multifactor optimization of the adsorption process. The Design Expert Version 13 software selects the factors necessary for the best results. Based on the data presented in Figure 4, it can be observed that specific parameters yield optimal results. These parameters are agitation period = 29.34 min, CeO_2 NP dose = 0.302 g/L, pH = 6.96, and RB dye initial concentration =88.7 mg/L. Utilizing these specific values achieved a maximum RB adsorption of 88.46%, resulting in a desirability score of 0.991. The predicted RB removal was validated by the experimental results obtained under the ideal conditions.

3.4 Adsorption Kinetics

Choosing an appropriate model for data analysis is crucial as it helps to model dye influx into adsorbent and gives a more detailed description of reaction pathways [16]. The adsorption kinetics of RB dye on CeO_2 NP were assessed through PFO and PSO models. Figure 5 **(A)** and **(B)** represent fitting plots of different adsorption kinetic models, and Table 4 presents kinetic parameters. The correlation coefficient (R^2) denotes the fitness of each model. In PFO kinetics, the model reports the overall rate at which adsorption through a system is proportional to its driving force. Lastly, the concentration differential between the initial and equilibrium dye concentrations is the driving force. An analogy of correlation coefficients between PFO (R^2 = 0.9865) and PSO (R^2 = 0.9936) kinetic models reveals that PSO best exhibits the mechanism and adsorption rate. The chemical process of electron sharing, or transfer, is known as an adsorption system [17].

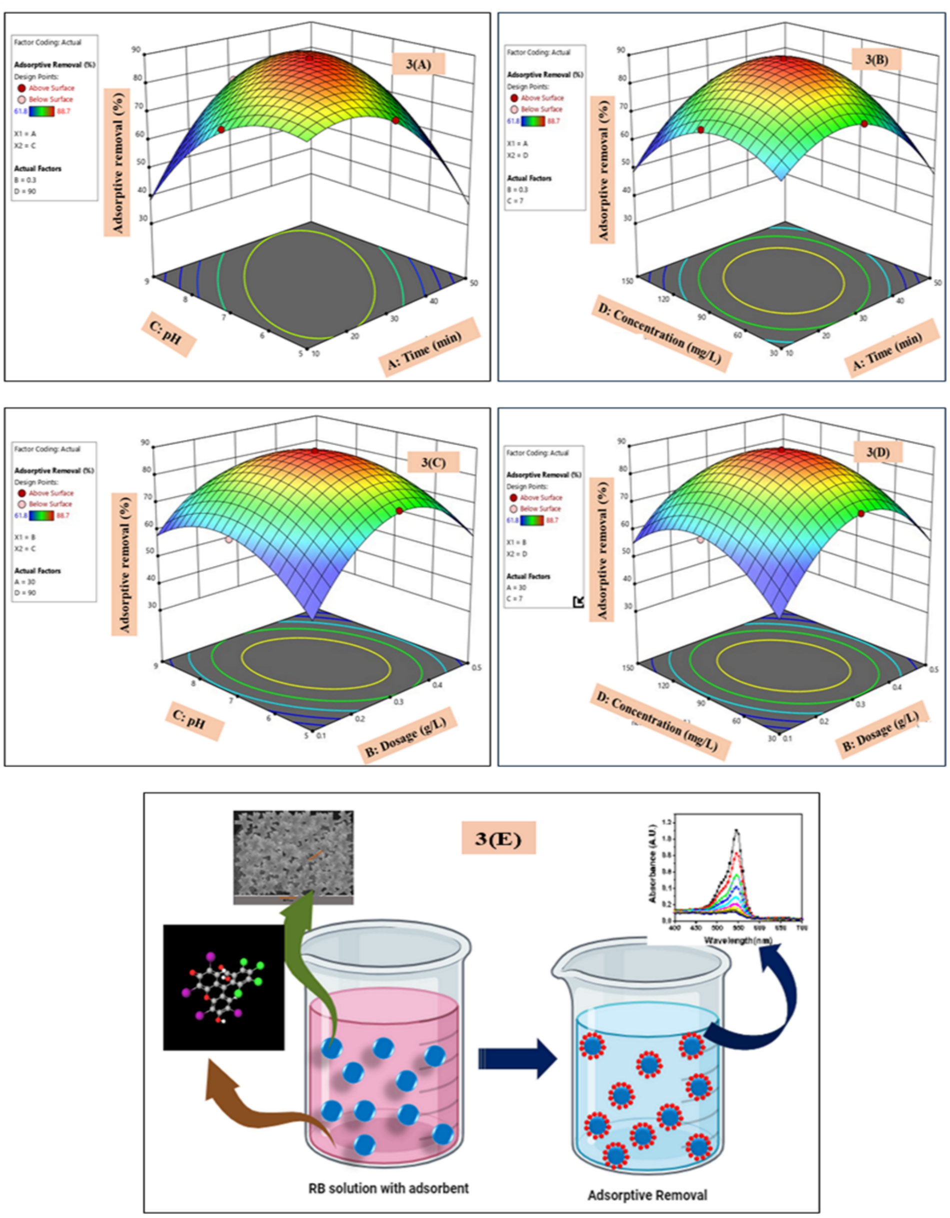

Fig 3. (A) Response surface plots for adsorption: interactional effects of Time and pH, (B) Response surface plots for adsorption: interactional effects of Time and Concentration, (C) Response surface plots for adsorption: interactional effects of pH and Dosage, (D) Response surface plots for adsorption: interactional effects of Dosage and Concentration, and (E) Schematic representation of adsorption of RB onto CeO_2

Table 4. Parameters of the PFO and PSO models for adsorption of RB dye

PFO model				PSO Model			
$q_e(Expt.)$	$q_e(Th.)$	K_1	R^2	$q_e(Expt.)$	$q_e(Th.)$	K_2	R^2
178	202	0.0695	0.9865	178	198	0.000018	0.9936

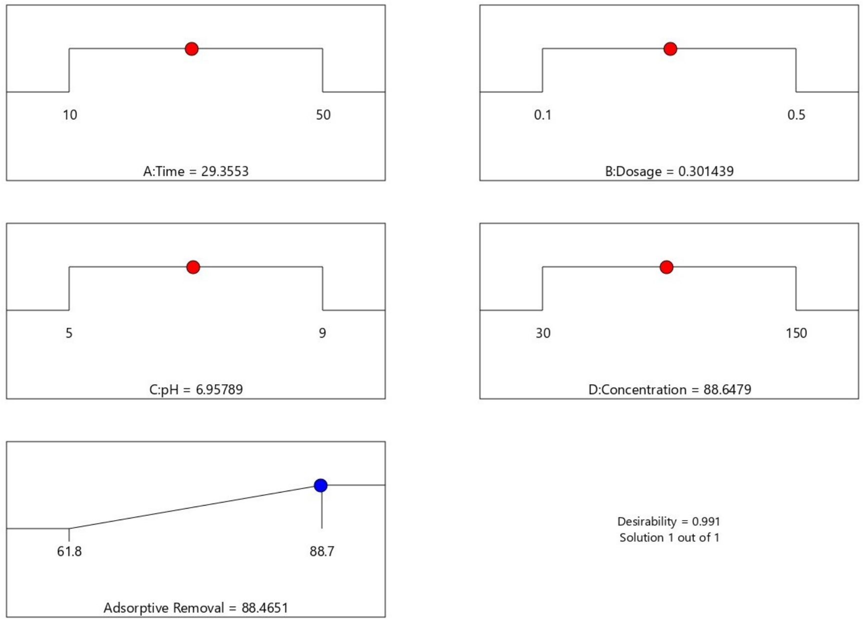

Fig 4. Ramp plot for optimizationof adsorption of RB onto CeO_2

3.5 Adsorption Isotherms

The process mechanism, adsorbent properties, and adsorbate-adsorbent interaction can be determined from the adsorption isotherms[18]. Consequently, the interpretation and prediction of adsorption data necessitate the correlation of equilibrium data. The Freundlich and Langmuir isotherm model fitting curves are depicted in Figure 5 **(C)** and **(D).** These figures show that the Freundlich model represents the adsorbed statistics more closely. This suggests that the adsorption process involves both monolayer and multilayer adsorption, and the adsorption sites are heterogeneous. When 'n', the exponent in the Freundlich equation, is greater than 1, it suggests a favorable adsorption process.

3.6 Adsorption Thermodynamics

The thermodynamic parameters may be determined using the data from Figure 5 **(E)**. The thermodynamic parameters that were determined are displayed in Table 5. Based on the negative ΔG values observed at different temperatures, it may be concluded that the adsorption process occurred spontaneously and was thermodynamically feasible[19]. Increasing temperature causes a modest drop in ΔG values, suggesting that more dye is absorbed into the adsorbent surface. As a result, higher temperatures promote RB dye absorption. Positive ΔH and ΔS values imply an endothermic nature and increased unpredictability at the solid-solution interface during adsorption[20].

Table 5. Thermodynamic parameters

Temp. (K)	ΔG (J/mol)	ΔH (kJ/mol)	ΔS (J.mol/K)
298	-407.65	40.33	136.93
303	-414.49		
308	-421.34		
313	-428.19		
318	-423.03		

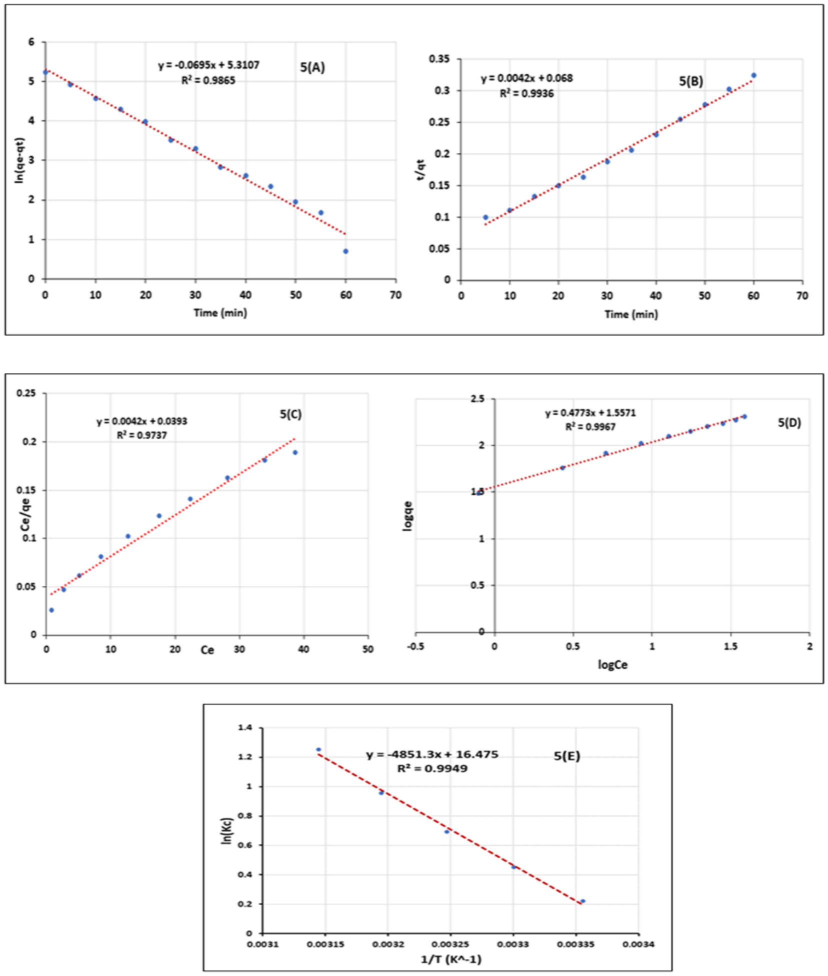

Fig 5. Kinetics, isotherms, and thermodynamics of adsorption of RB dye onto CeO_2: (A) pseudo-first-order model, (B) pseudo-second-order model, (C) Langmuir isotherm model, (D) Freundlich isotherm model, and (E) thermodynamics

4 Conclusion

The CeO_2 NPs were successfully synthesized using the coprecipitation method. The microstructural analysis showed that a flower-like nanocrystal was produced, and the particle size calculated from the XRD spectra was 44.8 nm. The band gap energy E_g was estimated to be 3.68 eV. The synthesized CeO_2 NPs were used as an adsorbent of RB dye from an aqueous solution. The RSM-CCD methodology was employed to evaluate the optimization of process parameters. The optimal RB adsorption of 88.46% with desirability of 0.991 was achieved using the agitation time of 29.36 min, NP dosage of 0.302 g/L, pH of the solution of 6.96, and initial RB dye concentration of 88.65 mg/L. The measured adsorption capacity of 178 mg/g good agreed with the maximum adsorption q_{max} =187 mg/g determined from the modified Freundlich isotherm. The PSO model most effectively represented the adsorption kinetics. Thermodynamic studies determined the endothermic and spontaneous character of the adsorption. In conclusion, the synthesized CeO_2 nanoflower is a promising adsorbent for removing organic dyes in wastewater and can be used in wastewater treatment.

Acknowledgment

The authors are thankful to the Department of Physics, Bankura University and Bankura Zilla Saradamani Mahila Mahavidyapith.

References

1) Hassan MG, Wassel MA, Gomaa HA, Elfeky AS. Adsorption of Rose Bengal dye from waste water onto modified biomass. *Scientific Reports*. 2023;13(1):14776. Available from: https://doi.org/10.1038/s41598-023-41747-5.
2) Sundararaman S, Kumar JA, Deivasigamani P, Devarajan Y. Emerging pharma residue contaminants: Occurrence, monitoring, risk and fate assessment-A challenge to water resource management. *Science of the Total Environment*. 2022;825:153897–153897. Available from: https://doi.org/10.1016/j.scitotenv.2022.153897.
3) Gupta SV, Ahmaruzzaman M. CeO2/Fe3O4/g-C3N4 nanohybrid for adsorptive removal of Rose Bengal from aqueous stream. *International Journal of Environmental Analytical Chemistry*. 2024;104(7):1517–1536. Available from: https://doi.org/10.1080/03067319.2022.2039649.
4) Tasker TL, Burgos WD, Piotrowski P, Castillo-Meza L, Blewett TA, Ganow KB, et al. Environmental and human health impacts of spreading oil and gas wastewater on roads. *Environmental science & technology*. 2018;52(12):7081–7091. Available from: https://doi.org/10.1021/acs.est.8b00716.
5) Rathi BS, Kumar PS. Application of adsorption process for effective removal of emerging contaminants from water and wastewater. *Environmental Pollution*. 2021;280:116995–116995. Available from: https://doi.org/10.1016/j.envpol.2021.116995.
6) Qumar U, Hassan JZ, Bhatti R, Raza A, Nazir G, Nabgan W, et al. Photocatalysis vs adsorption by metal oxide nanoparticles. *Journal of Materials Science & Technology*. 2022;131:122–166. Available from: https://doi.org/10.1016/j.jmst.2022.05.020.
7) Samuel MS, Ravikumar M, John JA, Selvarajan E, Patel H, Chander PS, et al. A review on green synthesis of nanoparticles and their diverse biomedical and environmental applications. *Catalysts*. 2022;12(5):459–459. Available from: https://doi.org/10.3390/catal12050459.
8) Singh KR, Nayak V, Sarkar T, Singh RP. Cerium oxide nanoparticles: properties, biosynthesis and biomedical application. *RSC advances*. 2020;10(45):27194–27214. Available from: https://doi.org/10.1039/D0RA04736H.
9) Gadore V, Singh AK, Mishra SR, Ahmaruzzaman M. RSM approach for process optimization of the photodegradation of congo red by a novel NiCo2S4/chitosan photocatalyst. *Scientific Reports*. 2024;14(1):1118. Available from: https://doi.org/10.1038/s41598-024-51618-2.
10) Nosrati H, Heydari M, Khodaei M. Cerium oxide nanoparticles: synthesis methods and applications in wound healing. *Materials Today Bio*. 2023;23:100823–100823. Available from: https://doi.org/10.1016/j.mtbio.2023.100823.
11) Muduli S, Behera SS, Mohapatra RK, Parhi PK, Sahoo TR. Efficient adsorption and antimicrobial application of bio-synthesized porous CeO2 nanoparticles. *Materials Science and Engineering: B*. 2023;290:116275–116275. Available from: https://doi.org/10.1016/j.mseb.2023.116275.
12) Mandal G, Bhattacharjee B. Biosynthesis of ZnO nanoparticles using the young fruit of Borassus flabellifer: Characterization and photocatalytic removal of biohazardous safranin-O dye using solar irradiation. . *The Scientific Temper*. 2024;15(2):2092–2098. Available from: https://doi.org/10.58414/SCIENTIFICTEMPER.2024.15.2.19.
13) Kumar R, Sharma P, Rose PK, Sahoo PK, Bhattacharya P, Pandey A, et al. Co-transport and deposition of fluoride using rice husk-derived biochar in saturated porous media: Effect of solution chemistry and surface properties. *Environmental Technology & Innovation*. 2023;30:103056–103056. Available from: https://doi.org/10.1016/j.eti.2023.103056.
14) Manivannan N, Sycheva A, Kristály F, Muránszky G, Baumli P. Structural differences and adsorption behaviour of alkaline metals doped zinc oxide nanoparticles. *Scientific Reports*. 2022;12(1):2292–2292. Available from: https://doi.org/10.1038/s41598-022-06092-z.
15) Mandal G, Bhattacharjee B. Cerium Oxide Nanoparticle-Papain Enzyme Bioconjugate: Synthesis, Characterization and Optical Absorption Study for Biomedical Applications. *Indian Journal of Science and Technology*. 2024;17(13):1331–1339. Available from: https://doi.org/10.17485/IJST/v17i13.270.
16) Gadekar MR, Ahammed MM. Modelling dye removal by adsorption onto water treatment residuals using combined response surface methodology-artificial neural network approach. *Journal of environmental management*. 2019;231:241–248. Available from: https://doi.org/10.1016/j.jenvman.2018.10.017.
17) Ghaedi AM, Karamipour S, Vafaei A, Baneshi MM, Kiarostami V. Optimization and modeling of simultaneous ultrasound-assisted adsorption of ternary dyes using copper oxide nanoparticles immobilized on activated carbon using response surface methodology and artificial neural network. *Ultrasonics sonochemistry*. 2019;51:264–280. Available from: https://doi.org/10.1016/j.ultsonch.2018.10.007.
18) Mahmoodi NM, Oveisi M, Bakhtiari M, Hayati B, Shekarchi AA, Bagheri A. Environmentally friendly ultrasound-assisted synthesis of magnetic zeolitic imidazolate framework-Graphene oxide nanocomposites and pollutant removal from water. *Journal of Molecular Liquids*. 2019;282:115–130. Available from: https://doi.org/10.1016/j.molliq.2019.02.139.
19) Ma CM, Hong GB, Wang YK. Performance evaluation and optimization of dyes removal using rice bran-based magnetic composite adsorbent. *Materials*. 2020;13(12):2764–2764. Available from: https://doi.org/10.3390/ma13122764.
20) Ebisike K, Okoronkwo AE, Alaneme KK, Akinribide OJ. Thermodynamic study of the adsorption of Cd2+ and Ni2+ onto chitosan-Silica hybrid aerogel from aqueous solution. *Results in Chemistry*. 2023;5:100730–100730. Available from: https://doi.org/10.1016/j.rechem.2022.100730.